JOURNAL OF THERMOPHYSICS AND HEAT TRANSFER
Vol. 32, No. 2, April–June 2018

Technical Notes

Modeling of Pyrolyzing Ablation Problem with ABAQUS: A One-Dimensional Test Case

Yeqing Wang*
University of Florida, Shalimar, Florida 32579
Timothy K. Risch†
NASA Armstrong Flight Research Center, Edwards Air Force Base, California 93523
and
Crystal L. Pasiliao‡
U.S. Air Force Research Laboratory, Eglin Air Force Base, Florida 32542

DOI: 10.2514/1.T5274

Nomenclature

A	=	decomposing rate coefficient, 1/s
B'	=	normalized ablation rate, $\dot{m}_c/\rho_e U_e C_H$
C_p	=	specific heat, J/(kg · K)
E	=	activation energy, J/mol
h	=	enthalpy, J/kg
$\bar{h}$	=	mass weighted averages of the material enthalpy, J/kg
$\dot{m}_g$	=	pyrolysis gas mass flux, kg/(m^2 · s)
k	=	thermal conductivity, W/(m · K)
R	=	universal gas constant, 8.314 J/(mol · K)
$\dot{s}$	=	surface recession rate, m/s
T	=	temperature, K
t	=	time, s
y	=	in-depth direction coordinate, m
ε	=	emissivity coefficient
ρ	=	density, kg/m^3
$\rho_e U_e C_H$	=	heat transfer coefficient, kg/(m^2 · s)
σ	=	Stefan–Boltzmann constant, W/(m^2 · s · K^4)
ψ	=	reaction order

Subscripts

c	=	char
e	=	freestream
g	=	pyrolysis gas
r	=	recovery
s	=	surface
v	=	virgin
w	=	wall
∞	=	background condition

Received 1 June 2017; revision received 26 September 2017; accepted for publication 27 September 2017; published online 27 October 2017.

*Postdoctoral Research Associate, Research and Engineering Education Facility. Member AIAA.
†Deputy Branch Chief, Aerostructures Branch.
‡Assistant Chief Scientist, Munitions Directorate. Senior Member AIAA.

I. Introduction

DURING hypersonic reentry, the outer surface of the heat shield [i.e., the ablating thermal protection system (TPS)] experiences extreme high temperature due to complex convective and radiative heating. With increasing temperature, pyrolyzing TPS material decomposes and then releases the pyrolysis gas. Meanwhile, the outer surface undergoes chemical reactions, including vaporization, nitridation, and oxidation, which leads to the progressive material removal (i.e., the ablation).

For the past several decades, the development of accurate simulation models to predict the thermal and ablative response of such pyrolyzing materials has been an interest in the ablation research community [1–8]. As a consequence, numerous corresponding computational codes have been successfully developed to date, such as the CMA code and the FIAT analysis tool. The common feature of these codes is that they use moving grid systems with the finite difference (or finite volume) method. However, the availability of these codes to the research community is often restricted. Moreover, these codes are limited to one-dimensional (1-D) geometries/configurations and thus may not fully capture the effects of the complex geometric features on the resulting thermal and ablative response. Recently, a few attempts have been made to model pyrolyzing ablation problems with finite element analysis (FEA) [5–7]. When compared with the finite difference (or finite volume) method, the finite element method provides improved computational capabilities due to the flexibility and enhanced applicability of the method, especially to complex geometries [5–7]. A few custom-written ablation codes based on a finite element method have been recently developed [5,6,9]. On the other hand, the recent improvements of the commercial general-purpose FEA programs (e.g., ABAQUS) have also allowed them to be used for modeling pyrolyzing ablation problems. Moreover, when compared with custom-written ablation codes, the commercial general-purpose FEA programs provide enhanced capabilities in the form of usability, pre- and postprocessing, mesh generation, flexibility, etc. [7]. However, the default heat transfer analysis in these commercial FEA programs only allows one to model the general heat transfer problem, in which the heat loss due to material decomposition and surface material removal are not considered. In this Note, we present a novel computational procedure with ABAQUS that enables us to model a 1-D pyrolyzing test case. The computational procedure is performed using the ABAQUS coupled thermal-displacement step with multiple user subroutines and the ALE adaptive remesh algorithm, which allows a tight coupling between the in-depth heat conduction considering the material decomposition and the progressive material removal. Moreover, the proposed procedure solves sequentially the temperature and the density change (i.e., the temperature is solved first and then used to calculate the density change afterward). In this note, the proposed FEA computational procedure is verified by comparing the predictions of the temperature and ablation histories of the pyrolyzing material with the predictions obtained from the well-validated ablation code FIAT.

II. Problem Formulations and Numerical Procedure

A. Problem Formulations of Ablation

The fundamental modeling equations for hypersonic reentry ablation problems have been well studied in the literature [2–6]. Here, we provide a brief review of these equations. First, the in-depth energy balance equation that considers the decomposition of pyrolyzing material for a 1-D ablation problem in a coordinate fixed in space is written as

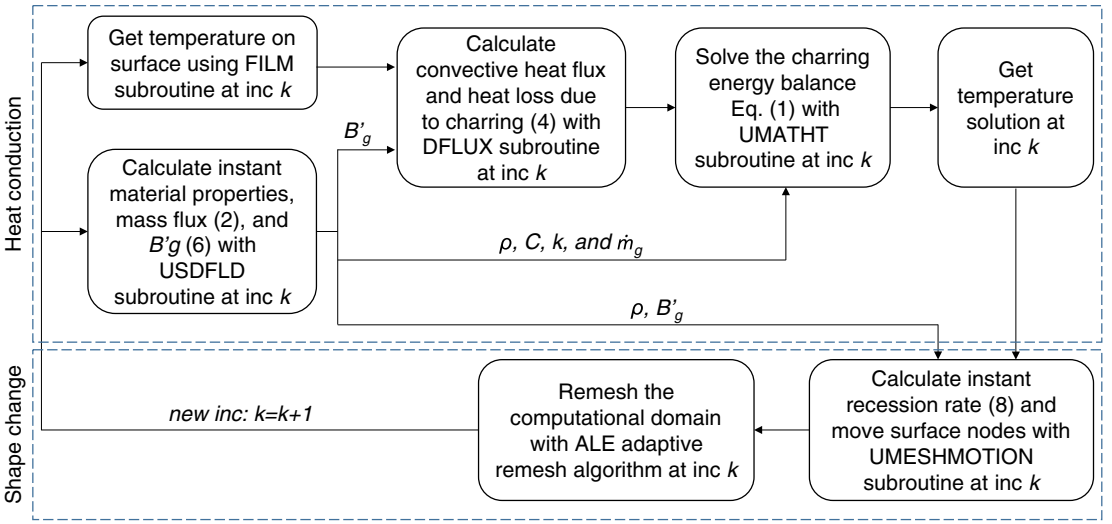

Fig. 1 Schematic of the proposed FEA procedure for solving pyrolyzing ablation problems with ABAQUS (where "inc" denotes time increment).

$$\rho C_p \left.\frac{\partial T}{\partial t}\right|_y = \frac{\partial}{\partial y}\left(k\frac{\partial T}{\partial y}\right) + (h_g - \bar{h})\left.\frac{\partial \rho}{\partial t}\right|_y + \dot{s}\rho C_p \frac{\partial T}{\partial y} + \dot{m}_g \frac{\partial h_g}{\partial y} \quad (1)$$

Note that the material properties (e.g., C_p, k, and h_g) are all functions of temperature or both temperature and pressure. The descriptions for these functions can be found in [5–7]. The pyrolysis gas mass flux $\dot{m}_g$, at any location y, in the case of a 1-D ablation problem, can be calculated using

$$\dot{m}_g = -\int_0^y \frac{\partial \rho}{\partial t}\,\mathrm{d}y \quad (2)$$

Here, the rate of density variation of the pyrolyzing material due to the decomposition of the resin components is typically expressed using the following equation:

$$\frac{\partial \rho}{\partial t} = -A\exp\left(-\frac{E}{RT}\right)\rho_v\left(\frac{\rho-\rho_c}{\rho_v}\right)^{\psi} \quad (3)$$

Second, the surface energy balance that considers the surface material removal of the pyrolyzing material during ablation is written as

$$-k\frac{\mathrm{d}T}{\mathrm{d}y} = \rho_e U_e C_H \cdot (h_r - h_w) + \rho_e U_e C_H \cdot (B'_c h_c + B'_g h_g - B' h_w) - \sigma\varepsilon(T_w^4 - T_\infty^4) \quad (4)$$

where B' is the total normalized ablation rate, that is,

$$B' = B'_g + B'_c \quad (5)$$

with B'_g being the normalized ablation rate due to pyrolysis gas liberation, and B'_c being the normalized ablation rate due to char consumption.

Here, the normalized ablation rate due to pyrolysis gas liberation B'_g can be calculated using

$$B'_g = \frac{\dot{m}_g}{\rho_e u_e C_H} \quad (6)$$

Once B'_g is calculated, the enthalpy of the gas phase just above the surface h_w and the normalized ablation rate due to char consumption B'_c can be obtained using the three-dimensional (i.e., with respect to pressure, temperature, and B'_g) B' look-up table [10]. After that, the normalized mass loss rate due to charring $\dot{m}_c$ is calculated using

$$\dot{m}_c = B'_c \cdot \rho_e u_e C_H \quad (7)$$

Finally, the surface recession rate $\dot{s}$ [i.e., the rate of surface material removal, see Eq. (1)] can be obtained using

$$\dot{s} = \frac{\dot{m}_c}{\rho_s} \quad (8)$$

B. Numerical Implementation with ABAQUS

The default heat transfer analysis provided in ABAQUS considers the general heat conduction scenarios without taking into account the heat loss due to the material decomposition for the pyrolyzing ablation problems and thus is insufficient to model the pyrolyzing ablation problems. Meanwhile, the default heat transfer analysis is unable to track the moving boundary condition due to surface material removal during ablation. Moreover, the default convective boundary condition that can be defined in the ABAQUS input is expressed as a function of surface temperature, whereas in the case of pyrolyzing ablation problems, the convective boundary condition is a function of enthalpy due to surface chemical reactions [see the first term on the right side of Eq. (4)]. To enable ABAQUS with the capability of modeling the pyrolyzing ablation problems, additional user subroutines must be provided.

The proposed FEA procedure is performed using the coupled thermal-displacement step in ABAQUS, and it is supplemented by five ABAQUS user subroutines and the ALE adaptive remesh algorithm (see schematic diagram in Fig. 1) [11]. Here, the FILM

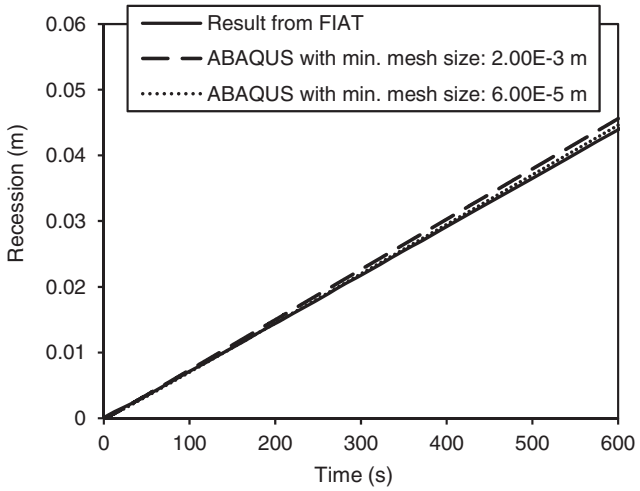

Fig. 2 Comparison of recession history between the predictions from ABAQUS (with two different sets of mesh size) and FIAT.

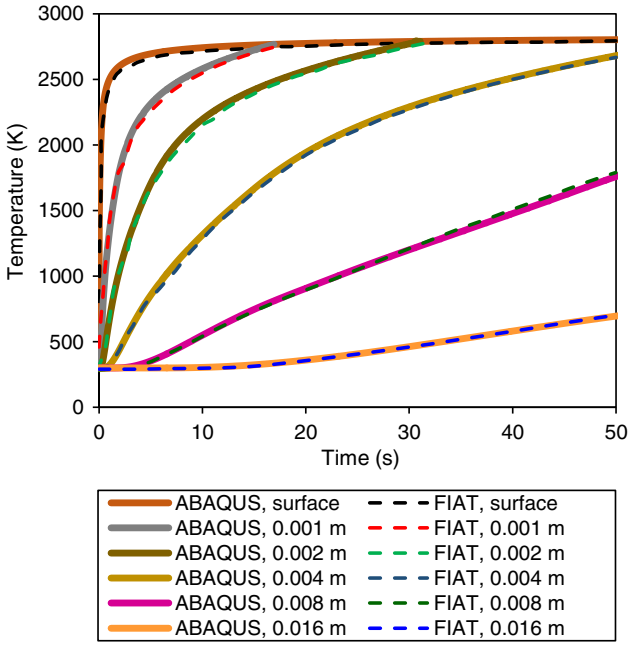

Fig. 3 Comparison of predicted temperature histories at surface and different depths of the material between ABAQUS and FIAT.

subroutine is used to obtain the temperature on the surface nodes at each time increment, whereas the USDFLD subroutine serves to update the material properties (e.g., thermal conductivity and specific heat), density change, mass flux, and B'_g after each time increment. Note that the integral in Eq. (2) (i.e., the pyrolysis gas mass flux) is computed using the trapezoidal rule (although a higher-order integration scheme could be used). The instant material properties and the temperature of the surface nodes are passed to the DFLUX subroutine to determine the surface boundary condition (4). Meanwhile, the heat generation considering material decomposition [Eq. (1)] is defined in the UMATHT subroutine. The temperature solution at each time increment is obtained by solving the governing equation (1) with surface boundary condition (4). Then, the temperature solution is transferred to the UMESHMOTION subroutine to calculate the instant recession rate [Eq. (8)] and the ablation depth. With the calculated instant ablation depth, the UMESHMOTION subroutine moves the surface nodes to their new locations. After that, the entire computational domain is remeshed with the ALE adaptive remesh algorithm and used to calculate the temperature solution for the next time increment. This procedure repeats until the last time increment, therefore enabling a tight coupling between the heat conduction considering material decomposition and the progressive shape change of the material. The data transfer between different user subroutines is achieved using common blocks provided by FORTRAN. Note that using common blocks in ABAQUS subroutines limits the proposed FEA procedure to a single CPU computational process (alternative methods need to be sought to allow for parallel computing).

III. Simulation Results and Verification

The pyrolyzing material considered in this Note is the theoretical ablative composite for open testing (TACOT) 3.0 test case material, where the material properties are listed with respect to temperature and pressure [10]. The material properties at a certain temperature and pressure are linearly interpolated during FEA with in-house developed FORTRAN utility subroutines. Note that the pressure is assumed to be constant at 1 atm in this study.

The thickness of the 1-D computational domain is 0.1 m. The upper surface of the material is exposed to a convective boundary condition with a heat transfer coefficient of 0.1 $\mathrm{kg}/(\mathrm{m}^2 \cdot \mathrm{s})$ and a recovery enthalpy of 40 MJ/kg. The bottom surface is adiabatic and the duration of the ablation is 600 s.

A. Numerical Accuracy: Effects of Mesh Size

To study the effects of mesh size on the numerical accuracy, two simulation cases are performed with two sets of mesh sizes. For both cases, fine meshes are used at the region near the heated surface (with minimum mesh sizes being 10×2 and 10×0.06 mm for the first and second case, respectively), whereas more coarse meshes are used at the region away from the heated surface (with maximum mesh sizes being 10×2 and 10×1 mm for the first and second cases, respectively). The average computational time is about 3 min on a laptop PC. The predicted recession histories using the proposed computational procedure for these two cases are compared with the results obtained from the well-validated 1-D finite-volume ablation code FIAT, developed by NASA Ames Research Center [2]. Figure 2 illustrates that the percentage error of ablation depth drops from 3.9 to 1.7% when the minimum mesh size is decreased from 2 to 0.06 mm. It should be noted that the percentage error may necessarily increase if the ablation duration extends, nevertheless, it can be mitigated with an even finer mesh. For a minimum mesh size of 0.06 mm, the

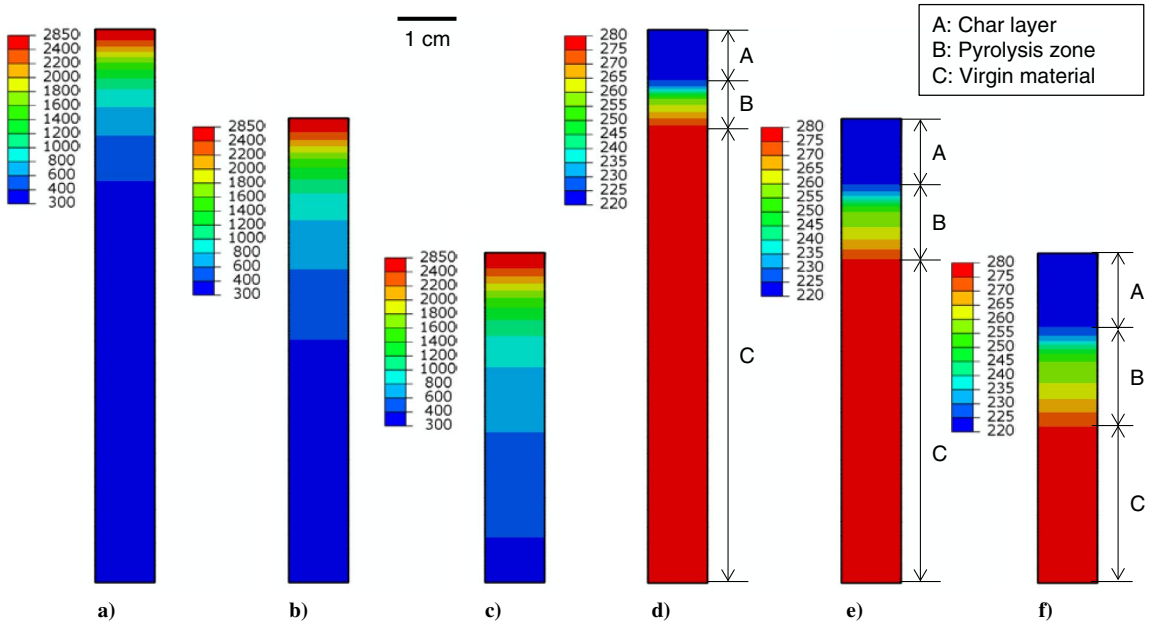

Fig. 4 Temperature distributions and ablation profiles at a) 100, b) 300, and c) 600 s and density distributions at d) 100, e) 300, and f) 600 s.

temperature results are presented in the following section. Here it is worth mentioning that, with such a minimum mesh size (and time increment), the sequential computational procedure provides quite accurate results in terms of global behavior.

B. Simulation Results and Verification

The temperature responses at the surface and depths of 0.001, 0.002, 0.004, 0.008, and 0.016 m are predicted with the fine mesh set (i.e., minimum mesh size of 0.06 mm) using the proposed FEA procedure. The predictions are compared with those predicted from FIAT, as shown in Fig. 3, and it can be seen that good agreement is achieved. In addition, Fig. 4 illustrates the temperature distributions and ablation profiles at 100 (Fig. 4a), 300 (Fig. 4b), and 600 s (Fig. 4c). Moreover, the status of material decomposition can also be visually observed by examining the density distributions of the material. Figures. 4d–4f provide the density distributions at 100 (Fig. 4a), 300 (Fig. 4b), and 600 s (Fig. 4c), where the region with density of 280 kg/m^3 (i.e., the virgin density) denotes the virgin material, the region with density of 220 kg/m^3 (i.e., the char density) denotes the char layer, and the region with density between 220 and 280 kg/m^3 denotes the pyrolysis zone.

IV. Conclusions

In this Note, a novel finite element analysis (FEA) computational procedure with ABAQUS has been proposed to predict the thermal and ablative response of the TACOT 3.0 test case (1-D) pyrolyzing material. The FEA procedure consists of multiple user subroutines and the ALE adaptive remesh algorithm, which enables a tight coupling between the heat conduction considering material decomposition and the progressive material removal. The predicted temperature and ablation histories using the proposed FEA procedure compare favorably with those predicted using FIAT (i.e., a well-validated pyrolyzing ablation code). It is also worth mentioning that the user subroutines of this proposed FEA procedure can be easily integrated as an add-on toolkit into ABAQUS, which would provide a more user-friendly modeling environment. The feasibility of extending the proposed FEA procedure to two- and three-dimensional pyrolyzing ablation problems will be investigated in future work.

The essence of this note is to demonstrate that a commercial finite element code, such as ABAQUS, can be used to perform ablation calculations. Currently, these calculations have required specialized custom-written codes and the advantages of using a commercial code have been demonstrated in other disciplines (e.g., structural and CFD). Future work will also investigate the effectiveness, limitation, and applicability of the proposed procedure for a broader range of ablation conditions.

It is also worth noting that, for relatively low-conductivity materials, the practice of using a 1-D ablation model is well documented and provides sufficient accuracy for initial sizing analysis. In this Note, the proposed 1-D ablation model decoupled the in-depth thermal response from the flowfield. To achieve more accurate predictions, the shape change needs to be coupled with the flowfield (i.e., the gas–solid boundary condition needs to be solved in a time-dependent manner). Although coupling the shape change to the external flow solver can be done, often times the change in the body geometry as a result of ablation is small, hence the decoupling of the flow and the in-depth thermal response. Even if the shape change is large, decoupled methods are still attractive because of the economy of calculation. Many current space vehicles are designed, at least initially, using a decoupled approach, even the Mars Science Laboratory vehicle [8]. Note that the procedure presented in this Note does not preclude the eventual coupling of the flowfield to the vehicle shape change due to ablation, instead, it is the first step in achieving this more ambitious goal.

Acknowledgments

This work was supported by the U.S. Air Force Research Laboratory (AFRL) under contract no. FA8651-08-D-0108 and task order no. 42. Any opinions, findings, conclusions, or recommendations expressed in this work are those of the authors and do not necessarily reflect the views of the AFRL. Y. Wang also thanks Joseph Koo (University of Texas at Austin) and Alexandre Martin (University of Kentucky) for their suggestion to examine the TACOT 3.0 ablation test case.

References

[1] Bartlett, E. P., Kendall, R. M., and Rindal, R. A., "A Multicomponent Boundary Layer Chemically Coupled to an Ablating Surface," *AIAA Journal*, Vol. 5, No. 6, 1967, pp. 1063–1071. doi:10.2514/3.4138

[2] Chen, Y. K., and Milos, F. S., "Ablation and Thermal Response Program for Spacecraft Heatshield Analysis," *Journal of Spacecraft and Rockets*, Vol. 36, No. 3, 1999, pp. 475–483. doi:10.2514/2.3469

[3] Chen, Y. K., and Milos, F. S., "Two-Dimensional Implicit Thermal Response and Ablation Program for Charring Materials," *Journal of Spacecraft and Rockets*, Vol. 38, No. 4, 2001, pp. 473–481. doi:10.2514/2.3724

[4] Chen, Y. K., and Milos, F. S., "Three-Dimensional Ablation and Thermal Response Simulation System," *38th AIAA Thermophysics Conference*, AIAA Paper 2005-5064, 2005.

[5] Dec, J. A., and Braun, R. D., "Three-Dimensional Finite Element Ablative Thermal Response and Design of Thermal Protection Systems," *Journal of Spacecraft and Rockets*, Vol. 50, No. 4, 2013, pp. 725–734. doi:10.2514/1.A32313

[6] Dec, J. A., Braun, R. D., and Lamb, B., "Ablative Thermal Response Analysis Using the Finite Element Method," *Journal of Thermophysics and Heat Transfer*, Vol. 26, No. 2, 2012, pp. 201–212. doi:10.2514/1.T3694

[7] Risch, T. K., "Verification of a Finite-Element Model for Pyrolyzing Ablative Materials," *47th AIAA Thermophysics Conference, AIAA AVIATION Forum*, AIAA Paper 2017-3354, 2017.

[8] Chen, Y. K., Gökçen, T., and Edquist, K. T., "Two-Dimensional Ablation and Thermal Response Analyses for Mars Science Laboratory Heat Shield," *Journal of Spacecraft and Rockets*, Vol. 52, No. 1, 2015, pp. 134–143. doi:10.2514/1.A32868

[9] Ewing, M. E., Richards, G. H., Iverson, M. P., and Isaac, D. A., "Ablation Modeling of a Solid Rocket Nozzle," *Fifth Ablation Workshop*, Univ. of Kentucky, Lexington, Kentucky, 2012, http://uknowledge.uky.edu/cgi/viewcontent.cgi?article=1035&context=ablation [retrieved 9 Oct. 2017].

[10] Van Eekelen, T., Martin, A., Lachaud, J., and Bianchi, D., "Test Case Series 3," *Ablation Workshop: Code Comparison*, Vol. 2, Univ. of Kentucky, Lexington, Kentucky, 2014, http://uknowledge.uky.edu/ablation_code/2 [retrieved 9 Oct. 2017].

[11] "ABAQUS User Subroutine Reference Manual," Ver. 6.14, ABAQUS, Providence, RI, 2014.